Journal of Hazardous Materials 192 (2011) 1623–1632

Contents lists available at ScienceDirect

Journal of Hazardous Materials

journal homepage: www.elsevier.com/locate/jhazmat

Analysis of concentration fluctuations in gas dispersion around high-rise building for different incident wind directions

X.P. Liu[a,b], J.L. Niu[b,*], K.C.S. Kwok[c]

[a] State Key Laboratory of Fire Science, University of Science and Technology of China, Hefei 230027, PR China
[b] Department of Building Services Engineering, The Hong Kong Polytechnic University, Hong Kong
[c] CLP Power Wind/Wave Tunnel Facility, Hong Kong University of Science and Technology, Hong Kong

ARTICLE INFO

Article history:
Received 15 February 2011
Received in revised form 29 June 2011
Accepted 29 June 2011
Available online 6 July 2011

Keywords:
Gas dispersion
High-rise residential building
Wind tunnel
Concentration fluctuations

ABSTRACT

This article presents experimental results that illustrate the unsteady characteristics of gas dispersion around a complex-shaped high-rise building for different incident wind directions. A series of wind tunnel experiments were conducted using a 1:30 scale model that represented the real structures under study. The objective of this paper is to study the behaviour of concentration fluctuations through transient analysis. Tracer gas was continuously released from a point source located at different positions, and a time series of fluctuating concentrations were recorded at a large number of points using fast flame ionization detectors. The experimental data were analysed to provide a comprehensive data set including variances and associated statistical quantities. Both the unsteady characteristics of the system and their potential practical impact are presented and discussed. Under crowd living conditions, the air pollutant exhausted from one household could probably re-enter into the neighbouring households, traveling with ambient airflow. Such pollutant dispersion process is defined as air cross-contamination in this study. The results indicate that the wind-induced cross-contamination around the studied type of high-rise building should not be overlooked, and the fluctuating concentrations should be paid attention to particularly during the evaluation of a potential contamination risk. This study can help deepen our understanding of the mechanisms of air cross-contamination, and will be useful for implementing optimization strategies to improve the built environments in metropolitan cities such as Hong Kong.

1. Introduction

The study of atmospheric dispersion around buildings has been the subject of extended research over the past several decades because of the increased concern for human health [1]. Pollutants of interest include the products of fires or accidental releases from nearby facilities, which can be harmful to the public if they penetrate into buildings. Contaminant distribution and transmission routes near buildings can be extremely complicated because of the interactions between released plumes and building structure. Numerous studies by employing both experimental [2] and simulation [3–5] methods have been conducted on the behaviour of plumes released near street level in built-up downtown areas. Reliable prediction of the pollutant concentration field near buildings is very important for building engineers to use in designing proper intake and exhaust locations to avoid unwanted consequences.

There exists a significant amount of work investigating the spread of a dispersing plume using a wide range of methods. Generally, there are two categories of methods used to study pollutant dispersion around buildings: experimental methods including full-scale measurements and scale modelling, and prediction methods including empirical models and computational fluid dynamics simulations. A comprehensive review [6] has been made of the methods that exist for predicting pollutant dispersion. Such studies often describe the concentration field in a time-averaged sense. However, the mean concentration field alone is not sufficient for estimating the potential hazard risk in cases such as an accidental release of a highly toxic pollutant near a building [7], or a flammable gas leakage [8]. It is therefore necessary to estimate not only the mean concentration of a pollutant but also concentration fluctuations. The detailed characteristics of the both mean concentration and concentration fluctuations of a plume dispersing through a large array of building-like obstacles have been illustrated by Yee and Biltoft [9] through a comprehensive series of field experiments. A cross-comparison was made by Gailis and Hill [10] using a wind tunnel study of a 1:50 scale model, and both these results were also compared with an open-terrain plume under similar conditions. The mean concentration and fluctuations of a dispersing plume in a street canyon have also been investigated by employing a wind tunnel method [11]. The unsteady

* Corresponding author. Tel.: +852 2766 7781; fax: +852 2774 6146.
E-mail address: bejlniu@polyu.edu.hk (J.L. Niu).

0304-3894/$ – see front matter © 2011 Elsevier B.V. All rights reserved.
doi:10.1016/j.jhazmat.2011.06.090

characteristics of a dispersing plume around an isolated building have also been studied by different approaches. Both experimental [12] and numerical methods [13] have been employed to study the concentration fluctuation of a plume around a cubic building model. Comparisons were also made between results obtained by different methods [14]. Aubrun and Leitl [15] used both field and wind tunnel methods to investigate the unsteady properties of a dispersion process in the vicinity of a building, and the good agreement between field and wind tunnel data confirmed that the instantaneous behaviour of the dispersion process could be modelled in a wind tunnel. Furthermore, aimed at a slightly more complex building shape, both wind tunnel [16] and field [17] experiments have been carried out to better understand the physical mechanisms of released plume dispersion around isolated buildings. These studies have been mostly limited to dispersion over a regular array of buildings or an isolated building with relatively simple shape.

The development of modern society calls for more understanding of pollutant transportation within complex building environments. New problems such as cross-contamination have been reported in our previous work [18], mainly focused on a pollutant originating from the building itself and its dispersion characteristics around a building under the buoyancy effect. Under crowd living conditions, the air pollutant exhausted from one household could probably re-enter into the neighbouring households, traveling with ambient airflow. Such pollutant dispersion process is defined as air cross-contamination in our study. It is necessary to further investigate such processes under more complicated situations. A wind tunnel investigation was therefore initiated to reveal the properties of the pollutant field around a typical high-rise building. In the present paper, emphasis is placed on concentration fluctuations. Time series of fluctuating concentrations were recorded at a large number of points which were located at the hypothetical positions of windows. The unsteady characteristics of the system were analysed on the basis of the fluctuation intensity and the cumulative distribution function (CDF). The 90th percentile values are also presented to illustrate the exposure risks from a practical point of view. Understanding the transient transport and dispersion of gaseous contaminants around complicated-shaped buildings is of both scientific and practical interest.

2. Methodology

2.1. Experimental arrangement

The equipment and methods used during the experiment have been thoroughly introduced in our previous paper [19]. In this paper, the arrangement is only briefly outlined, and particular attention was paid to the quality assurance of the statistical results.

The boundary layer flow was generated in the wind tunnel with a power law wind velocity profile having an exponent of 0.2. The turbulence intensity profile of the approaching wind flow was simulated in accordance with Terrain Category 2 stipulated in the Australian/New Zealand Standard [20]. The approach velocity measured in the wind tunnel at building height (1 m at model scale) was 3.27 m/s, so that the building Reynolds number exceeded 15,000 [21], ensuring that the measurement results were independent of the Reynolds number. A 1:30 scale model was constructed to represent a 10-story high-rise residential (HRR) building 30 m tall in prototype. The floor plan of the building is in a cross shape (#), and each floor contains eight units. Consequently, four semi-closed, so-called re-entrant spaces are formed in each high-rise block, into which the exhaust air from all the floors is discharged. This process can lead to a high possibility of cross-contamination. The tracer gas used was air with a 99,000 ppm propane concentration. The

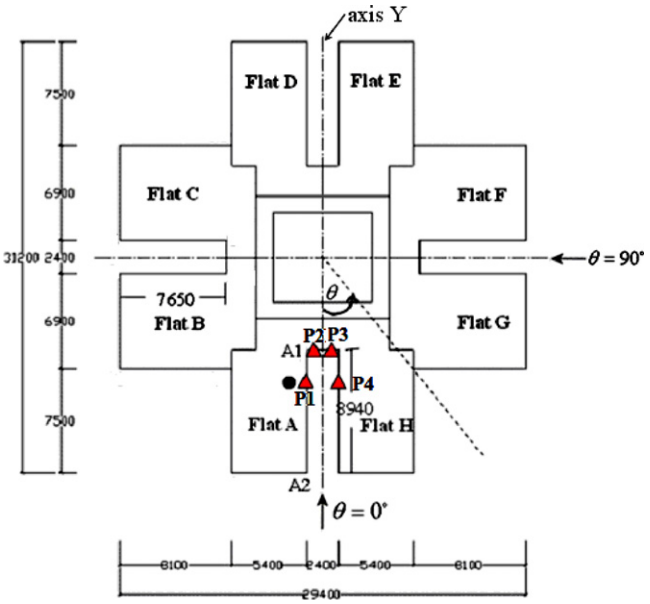

Fig. 1. Plan view of the building model (dimensions in mm) with the tracer gas source and measurement locations (source position: ●; measurement points: ▲).

tracer gas was released from a flow-meter at a constant flow rate (58.5 ml/s), and the nozzle exit was flush with the building surface. The tracer gas sources were located in façade A1–A2 at the 3rd floor, the 6th floor and the 9th floor, respectively, as shown in Fig. 1, at a point representing the normal position of toilet exhaust air. The four measurement locations at the height of each floor represent where windows are usually located. The wind direction was represented by θ, defined as the angle between the wind direction and the axis Y of symmetry of the building plan. The detection of tracer gas concentrations was achieved with a fast flame ionization detector (FID) model HFR400, on the basis of a careful calibration process using synthetic air and certified calibration gases of different concentrations. At each measurement position, sample air was collected via sampling tubes over a period of 120 s at a data-acquisition rate of 150 Hz.

As summarized in Table 1, all the testing cases were first conducted with four wind directions under closed-window conditions. All the cases were then repeated under open-window conditions. In the building model, four of the eight units (Flats A, B, H and G) in each floor have been designed to have openable windows with effective open areas equal to 50% of the real window size. According to the relevant building regulations in Hong Kong [22], a window's area should be at least equal to 1/16th of the floor area of the room for the purpose of natural ventilation. Therefore, the window-to-floor area ratio for the present model is controlled at approximately 7.4%. The window's locations and sizes are shown in Fig. 2, while the height of each of the windows is 900 mm (in prototype).

2.2. Quality assurance of statistical results

For statistical analysis of the concentration data, Aubrun and Leitl [15] have evaluated the influence of the averaging time on the statistical results through comparisons between wind tunnel experimental data and field measurement results. A dimensionless averaging time $T_a^* = T_a/(L_{ref}/U_{ref})$ was used, where T_a is the absolute averaging time, and L_{ref} and U_{ref} are the reference length and wind velocity, respectively. Compared with fully converged statistical results ($T_a^* = 36,000$), it was found that when the averaging time satisfied $200 < T_a^* < 400$,

Table 1
The configuration of each case (closed window).

Case no.	E1	E2	E3	E4	E5	E6	E7	E8	E9	E10	E11	E12
Source location	3rd Floor	6th Floor	9th Floor	3rd Floor	6th Floor	9th Floor	3rd Floor	6th Floor	9th Floor	3rd Floor	6th Floor	9th Floor
Orientation	$\theta = 0^\circ$	$\theta = 0^\circ$	$\theta = 0^\circ$	$\theta = 180^\circ$	$\theta = 180^\circ$	$\theta = 180^\circ$	$\theta = 45^\circ$	$\theta = 45^\circ$	$\theta = 45^\circ$	$\theta = 90^\circ$	$\theta = 90^\circ$	$\theta = 90^\circ$

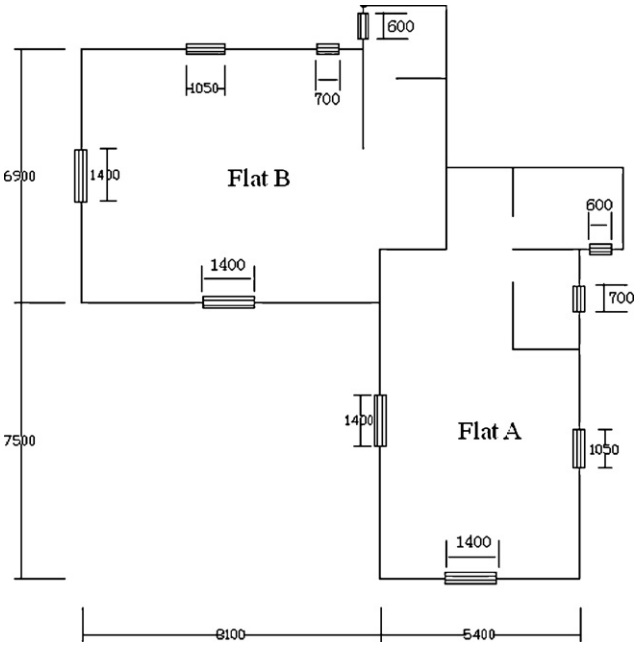

Fig. 2. Detailed window size and positions.

the experimental relative error for the statistical results was acceptable. With regard to the present experiment, the T_a^* calculated on the basis of a 120 s averaging time is approximately 390.

To further check the reliability of the results, a beforehand analysis was performed to estimate the minimum sampling time from specific tests. The minimum averaging time to reach a converged (i.e. representative) standard deviation is roughly 60 s and 90 s at selected key measurement points under closed- and open-window conditions, respectively, as shown in Fig. 3. It can be seen that the required time under open-window conditions is generally longer than that under closed-window conditions because the detected concentration could be more fluctuating when the window is open. Even at several special measurement points such as D0–S3–F4–P2 (■), which is located on the deep side of the re-entrant space, and D0–S6–F7–P1 (▲), which is located on the vertical adjacent floor near to the source location, a 90 s sampling time is sufficient to reach a converged standard deviation. Therefore, a 120 s sampling/averaging time additionally ensured an acceptable repeatability in the fluctuation results.

3. Results and analysis

The fluctuation intensity, cumulative distribution functions and 90th percentile values are presented and analysed here. It should be pointed out that a significantly large amount of data has been obtained during the experiment. The corresponding results, however, are not entirely discussed in this paper.

3.1. Concentration fluctuation intensity

The concentration fluctuation intensity is defined as $i = \sigma_c / C_{mean}$, where σ_c is the standard deviation and C_{mean} the mean concentration. Concentration fluctuation intensity is a useful statistic to quantify the level of fluctuation of the instantaneous plume concentration around the mean concentration. After examining the mean concentration data, in general it was found that when the contaminant source was located on the 3rd floor, the two vertically adjacent units were the most significantly influenced. When the source was located on the 6th floor, the influence region extended to three vertically adjacent floors. Therefore, the concentration fluctuation intensities of the adjacent two floors are presented (Fig. 4) when the source was located on the 3rd floor, while that of the adjacent

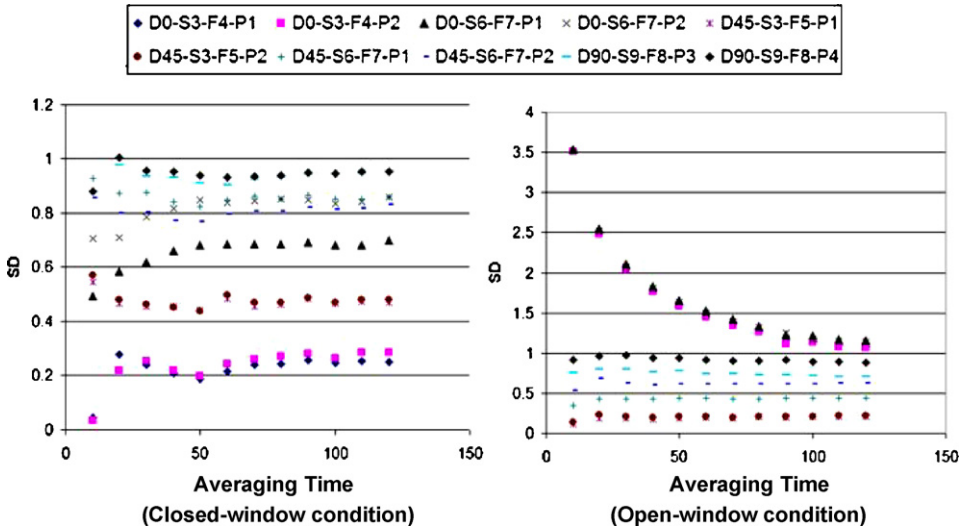

Fig. 3. Standard deviation versus averaging time. (The abbreviations "D", "S", "F" and "P" represent the wind incident angle, source location, measurement floor and measurement point, respectively.)

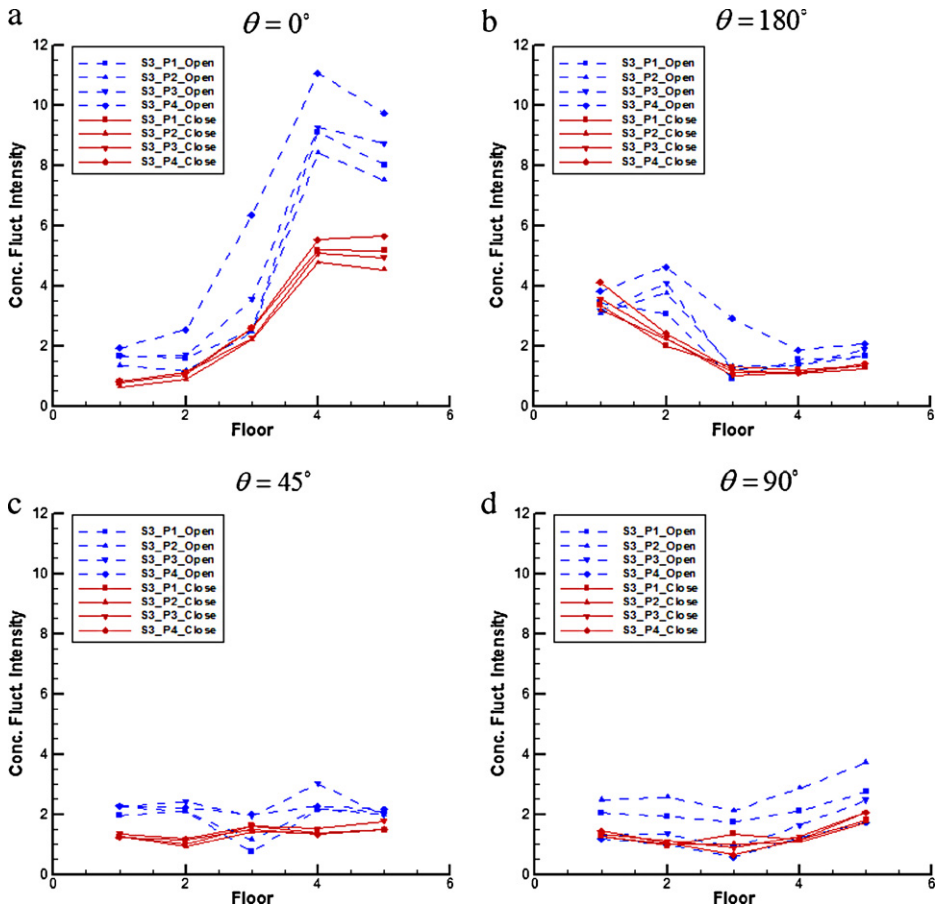

Fig. 4. Concentration fluctuation intensity when source was located on the 3rd floor.

three floors are presented when the source was located on the 6th floor (Fig. 5).

First it should be noted that, for most of the points, the values of the concentration fluctuation intensity were greater than 1, suggesting the fluctuations in instantaneous concentration were at least of the same values as the actual mean concentrations. It should be noted that the fluctuation intensity in the vertical direction varied with both the source location and the wind direction, because of the complicated interaction between the building and the boundary layer flow. Fluctuation intensity is clearly different from that of an open-terrain plume, as illustrated by Mylne [23] in his field experiments. Under open-terrain conditions, with a range of source heights, the downwind concentration fluctuations in the vertical direction generally increased with height. Yassin et al. [24] examined the vertical profiles of the concentration fluctuation at different downwind distances of an isolated high-rise building model, when the tracer gas was released from a ground level source located behind the model. It was found that the fluctuation intensity decreased along with the height, which is similar to the results shown in Figs. 4b and 5b, which show that the fluctuation intensity generally decreased from the lower floors to the higher floors when $\theta = 180^{\circ}$. Combining these results with the mean concentration distributions [19], it can be found that fluctuation intensities gradually increase towards the edges of the plume, where the mean values were relatively low, indicating less complete mixing farther away from the source as clear parcels of air were entrained within the plume structure. As shown from the results, the fluctuation intensity varied in a small range in cases E7 (Fig. 4c), E10 (Fig. 4d), E2 (Fig. 5a) and E8 (Fig. 5c), and varied widely in the other cases. Under the same wind direction, for example, comparing cases E1 (Fig. 4a) and E2 (Fig. 5a), the fluctuation intensities near the source floor were nearly constant when the source was located on the 6th floor. This is because the wind flow comes to the windward wall and rests halfway up the building to form a front stagnation region, which resulted in fluctuation intensities remaining constant in height. However, when the source was located on the 3rd floor, the tracer gas could be transported downward because of the generated upwind vortex, which results in the fluctuation intensities generally increasing with height (Fig. 4a).

The fluctuation intensity was larger at each measurement point under open-window conditions. In closed-window conditions, the fluctuation intensities were generally less than two at most points, while they were up to twice as large when the windows were open. Furthermore, the concentration fluctuation intensity was nearly uniform on each of the building façades on the same floor when the windows were closed, but differed under open-window conditions. These results indicate that the flow is more complex and more turbulent under open-window conditions because of the stronger mixing effect introduced by cross-ventilation. The figures also reveal that the distributions of concentration fluctuation under different window opening conditions are relatively similar. This result is consistent with the turbulence scales generated by the interaction of the building with the flow, which are mainly dominated by the building structure.

3.2. Cumulative distribution function

Another important parameter presented here is the CDF of each concentration time series [16]. The CDF represents the proportion of concentration readings within a time series that lie below a given

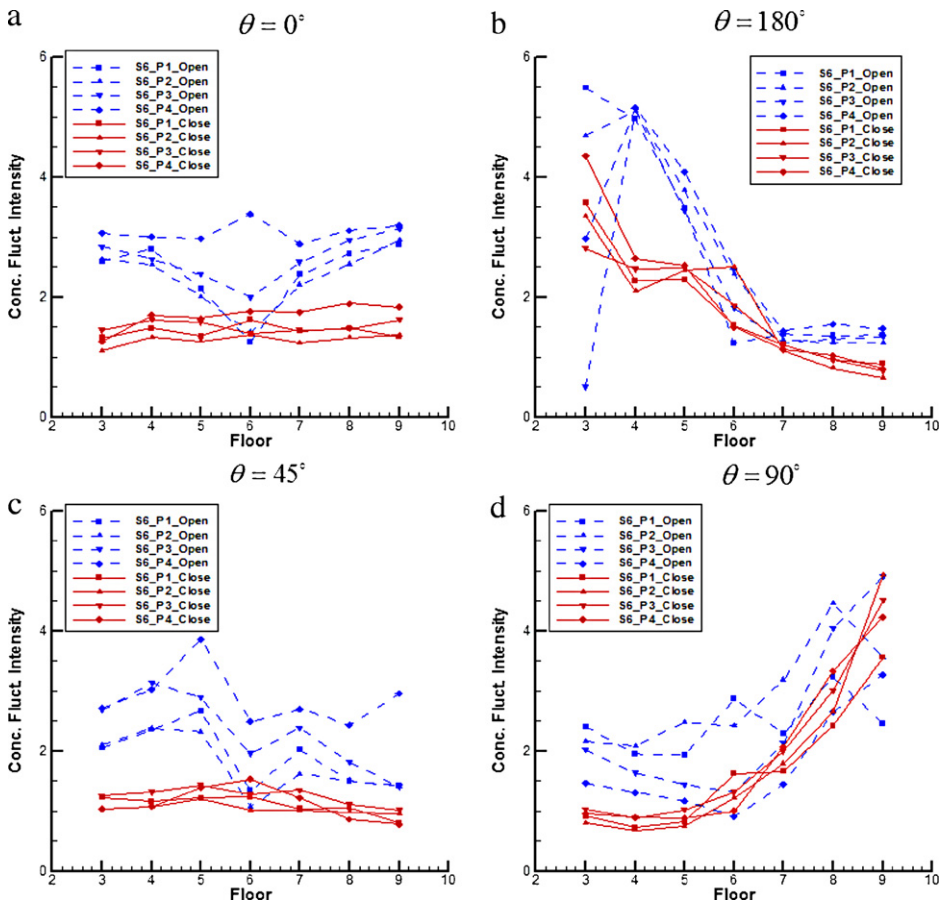

Fig. 5. Concentration fluctuation intensity when source was located on the 6th floor.

concentration (expressed as the ratio between the instantaneous and mean concentration values). The CDF provides the following information [17]: (a) the concentration fluctuation intensity, which is indicated by the slope of the central part of the curve (the lower the intensity the steeper the gradient); (b) intermittency, which is indicated by the intercept on the vertical axis; and (c) the ratio between peak and mean obtained, which is obtained from the *x*-value at which the CDF reaches 1. The definition of intermittency is the proportion of the concentration time series for which the concentration is at or below a threshold value, which in this case is the zero concentration. When the source was located in the middle of the building, the measured mean concentrations were relatively higher compared with the results from other source locations, which deserve further analysis. Therefore, the results presented here were first derived from data in which the source was located on the 6th floor, under $\theta = 0^\circ$ and $\theta = 180^\circ$, followed by a direct comparison between the other two wind directions.

Fig. 6b presents the progression of the CDF shape on vertically adjacent floors when the source was located on the 6th floor under closed-window conditions. The time series for one of the selected points are also presented in Fig. 6a for comparison purposes. First, it can be seen that the basic fluctuation features at each measurement point are clearly revealed through the CDF shape. For example, as shown in Fig. 6b3, the intermittency factors for points located on the 5th floor when $\theta = 180^\circ$ are greater than 0.7, while they are approximately 0.2 in other positions (as shown in Fig. 6b1, b2 and b4). This occurrence is also reflected by the concentration time series data; for points on the 5th floor when $\theta = 180^\circ$ the concentration value is nearly zero for about 70% of the sampling period, as shown in Fig. 6a3. It is additionally shown that both the fluctuation intensity and the peak-to-mean ratio at these points are relatively large, because of the comparatively low value of the mean concentration obtained at that floor.

Second, the CDF shapes are very similar at different measurement points on the same floor, indicating similar concentration fluctuation characteristics at the same floors. With regard to the different floors (Fig. 6b1 and b2), the CDF shapes are very much alike between the upper and lower floors. This suggests that the cumulative distribution frequencies of concentration fluctuation in the vertical direction are basically symmetric from the source floor when $\theta = 0^\circ$. With regard to different building orientations, the shapes of the CDF on the 5th floor are obviously different under $\theta = 0^\circ$ and $\theta = 180^\circ$ (as shown in Fig. 6b1 and b3), while they are similar on the 7th floor when compared between b2 and b4. This result is probably attributed to the vertical vortices generated at the leeward wall with flow direction from bottom to top. This situation results in the concentration data obtained on the 5th floor becoming more intermittent when $\theta = 180^\circ$.

Fig. 7 shows the CDF shapes of selected floors when $\theta = 0^\circ$ and $\theta = 180^\circ$, under open-window conditions. It can be seen that the overall CDF shapes are slightly different compared with the results obtained under closed-window conditions. When the windows are open, the concentration data are highly intermittent, and the intermittency factors obtained under $\theta = 0^\circ$ range up to 0.6. When $\theta = 180^\circ$, as shown in Fig. 7c and d, both the intermittency factor and peak-to-mean ratio are also larger than that shown in Fig. 6b3 and b4. These results further reveal that the concentration fluctuation is more severe under open-window conditions.

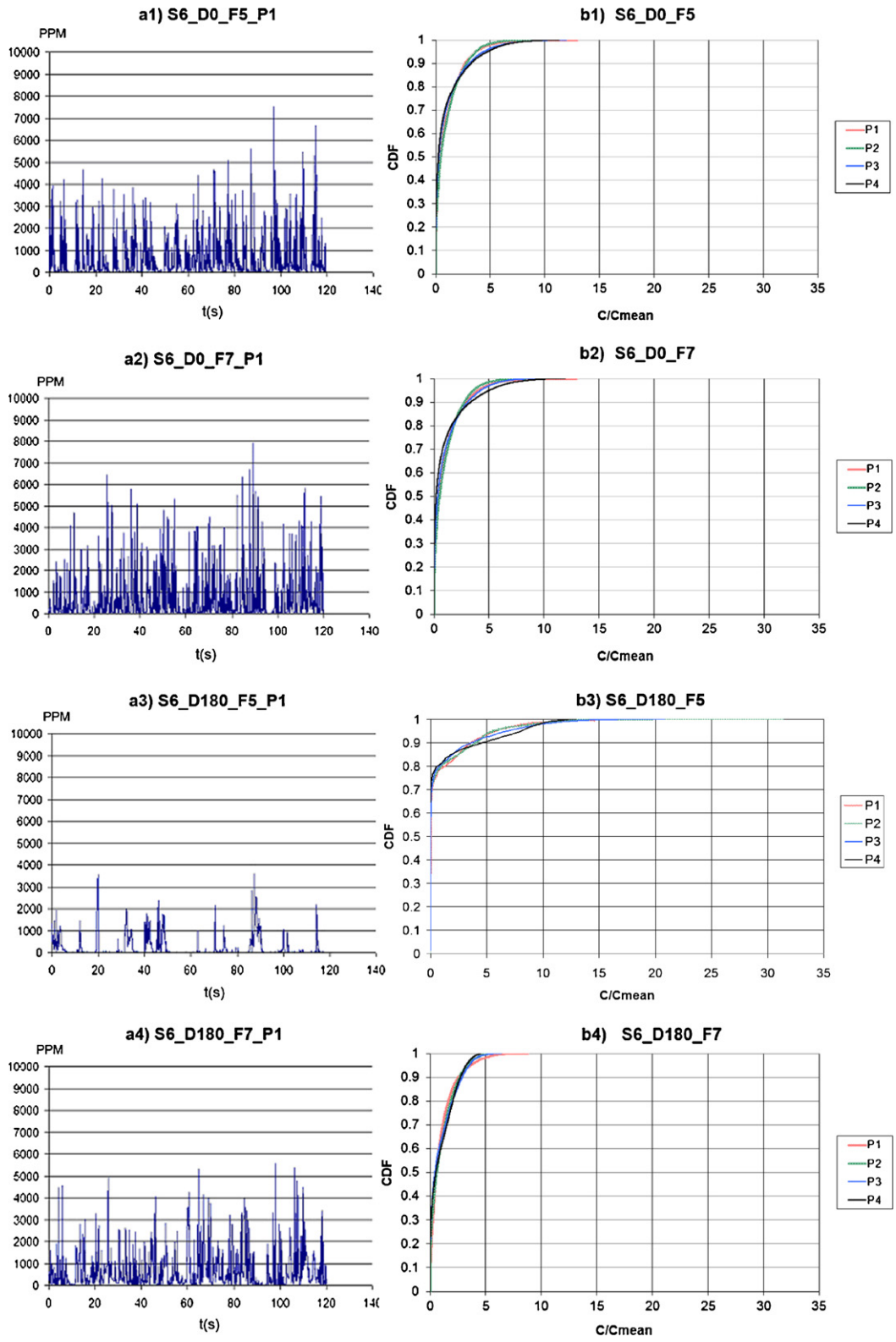

Fig. 6. Time series for point P1 and CDF shapes of P1 to P4 on vertical adjacent floors with closed-window condition. (The abbreviations F5 and F7 represent the 5th floor or the 7th floor, respectively.)

It should be noted that comparable differences also exist under open-window conditions. Comparing Fig. 7a and b, the CDF shapes are also very much alike between the vertical upper and lower floors, and the results for different measurement points on the same floors are close. With regard to different building orientations, on the 5th floor when $\theta = 180^{\circ}$, the CDF shape also shows a long gentle slope characteristic of a highly fluctuating region of flow with a comparatively high peak-to-mean ratio, while the intermittency is about 0.8. This result suggests that the differences between basic fluctuation features compared between measurement points are not significantly different when the windows are opened, at least for the present cases.

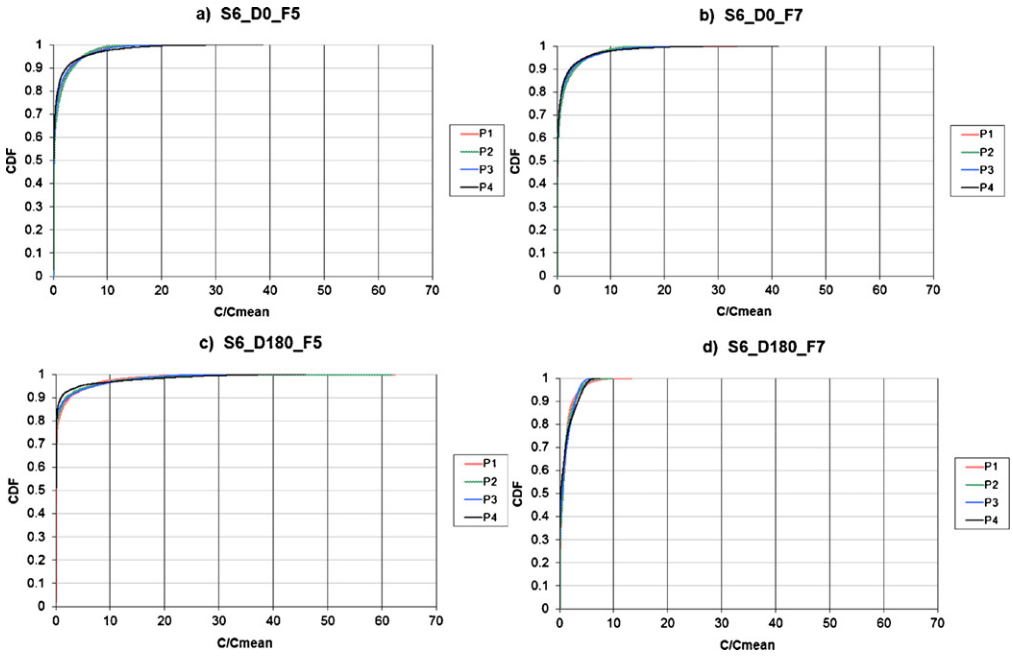

Fig. 7. CDF shapes on vertical adjacent floors with open-window condition. (The abbreviations F5 and F7 represent the 5th floor or the 7th floor, respectively.)

Fig. 8 shows comparisons of CDF at the same measurement points under two wind directions ($\theta = 45^\circ, \theta = 90^\circ$) with closed windows. It can be seen that when the incident angle is $\theta = 45^\circ$, the fluctuation intensity of the point P1 on the adjacent upper floor is higher than that of $\theta = 90^\circ$ (as shown in Fig. 8b), but on the adjacent lower floor it was lower than that of $\theta = 90^\circ$ (as shown in Fig. 8a). Comparing different CDF shapes, the intermittency factor at point P1 on the 7th floor under $\theta = 90^\circ$ is the largest, which indicates that during 40% of the sampling time the concentration level detected at that point is near zero.

Both the concentration fluctuation intensity and the CDF presented above illustrate the fundamental characteristics of the concentration fluctuations. With respect to hazard assessment, the following analysis is based on "instantaneous" concentration values, to further investigate the practical impact induced by the fluctuations.

3.3. 90th percentile values

Usually, for the target building, kitchen and bathroom windows are opened towards the re-entrant space into which exhaust air from all the floors is discharged, such as cooking odours generated from cooking processes. Taking into account concerns of odour annoyance, the 90th percentile values (the concentration levels exceeded 10% of the time) are presented here. These values give a clearer indication of where the high peak values occur than the intensity does. To study such dispersion processes, important parameters that can lead to an experience of annoyance depend upon the "instantaneous" concentration level over a time scale related to human breath. The temporal behaviour of the dispersion process should be captured and analysed over a time scale as small as one inhalation period (between 1 and 2 s). Thus, the original data-acquisition rate of 150 Hz is not required. Therefore, the 90th percentile values were calculated using 2 s-averaged (prototype) data. The 90th percentile values can be used to examine high concentration levels and to evaluate whether these can lead to an experience of odour annoyance. The definition of an odour unit per volume (1 OU m^{-3}) is associated with odorant concentration. A threshold value is the concentration of a substance that can be detected by half of the people present. However, this concentration level varies from person to person depending on their sensitivity to odours, and it is also different for various kinds of odorous substances. Thus, the key parameter used to evaluate the odour concentration level is actually the dilution factor. In this section, the 90th percentile values are presented in the following two ways: first, they are normalized by the mean concentration at each point to evaluate the high-concentration effect and the degree of its deviation from the local mean at each individual point; and second,

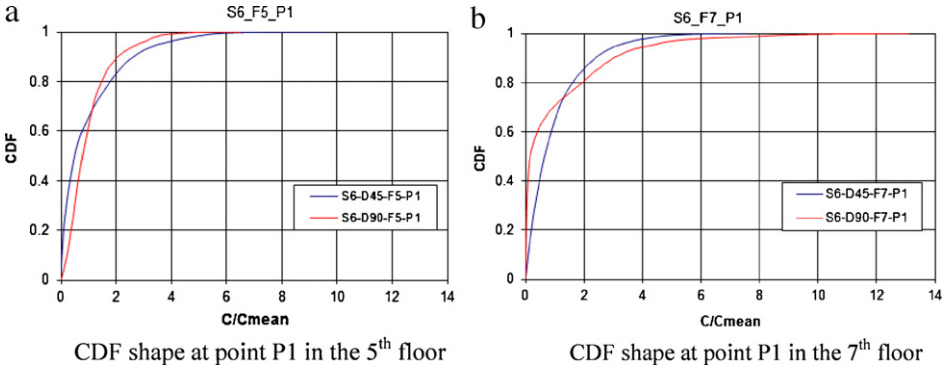

Fig. 8. CDF shapes under the other two wind directions ($\theta = 45^\circ, \theta = 90^\circ$).

Table 2
The 90th percentile normalized by mean concentration of each point (source located on the 6th floor, with closed windows).

Floor	$\theta = 0^\circ$				$\theta = 180^\circ$				$\theta = 45^\circ$				$\theta = 90^\circ$			
	P1	P2	P3	P4	P1	P2	P3	P4	P1	P2	P3	P4	P1	P2	P3	P4
3	2.7	2.6	2.9	2.6	1.9	2.2	2.1	2.1	2.6	2.5	2.4	2.2	2.3	2.2	2.4	2.2
4	2.8	3.0	3.0	3.3	3.9	4.2	3.3	4.3	2.5	2.6	2.5	2.4	2.0	1.9	2.2	2.2
5	2.6	2.8	2.9	3.2	3.7	4.1	3.8	4.6	2.5	2.6	2.7	2.4	2.0	2.0	2.4	2.3
6	2.8	2.9	3.1	3.5	2.5	3.6	4.3	3.6	2.2	2.3	2.6	2.5	2.6	2.5	3.0	2.4
7	2.8	2.7	2.9	3.2	2.5	2.6	2.7	2.7	2.3	2.3	2.3	2.1	3.1	3.3	3.5	4.4
8	2.7	2.6	2.8	3.1	2.3	2.2	2.2	2.5	2.3	2.2	2.2	1.9	3.6	3.1	2.9	2.2
9	2.5	2.6	2.7	2.8	2.1	1.9	2.0	2.1	1.9	2.2	2.1	1.8	1.9	1.7	2.1	2.3

they are normalized by the source concentration to give direct information about the dilution level and the frequency of exposure.

The 90th percentile values non-dimensionalized by the mean concentration are presented in Table 2 under different wind directions when the source is located on the 6th floor and windows are closed. As shown from the results, this ratio does not show a large variation in the studied region, and generally ranges from two to five in the presented cases. In the wind tunnel experiment conducted by Aubrun and Leitl [15], it was found that factors between these 90th percentile values and the mean concentration were less than four at most positions located in the vicinity of a pig barn. It can be observed that the ratio fluctuates around 2.8 when $\theta = 0^\circ$, while it fluctuates around 2.3 when $\theta = 45^\circ$. This result suggests that the levels of turbulence in the latter case are slightly lower than those of the former. This result is expected in view of the fluctuation intensity values presented earlier, as shown in Fig. 5a and c (cases E2 and E8, respectively). Furthermore, it should be noted that the ratio is nearly constant in both cases mentioned above, while it varies over a wider range in the other two cases studied, in which the re-entrant spaces did not face into the wind and can be treated as a "transposed canyon", to some extent. Pavageau and Schatzmann [11] showed a variable value ranging from 1.5 to 6 for the ratio of the 99-percentile value over the mean concentration, described in their wind tunnel studies aimed at studying dispersion in a street canyon, while corresponding simulation studies also showed similar results (from 1.5 to 5) [25].

When assessing the impact of odours, it is important to study both the concentration of odours and their frequency of occurrence. Examination of the spatial distribution of this 90th percentile is also useful to estimate the concentration level at each location affected by the source. Table 3 gives the 90th percentile values normalized by source concentration. When the odour concentration at the source location was known, the values and positions of short duration peaks could therefore be estimated to check for critical thresholds being exceeded. It can be observed from the results that even several floors away from a source the calculated 90th percentile ratio factor can remain larger than 1% in both vertical directions. In some positions such as points opposing the index unit, the 90th percentile concentration can reach one order of magnitude lower than the source concentration. These results directly illustrate the impact of the source location. For example, when exhaust air is released from one household during cooking processes, at a concentration equal to 1000 OU m^{-3}, the 90th percentile concentration obtained in several adjacent households could be several odour units per cubic meter under the given values. Thus, the possibility of causing odour annoyance can be estimated based on the concentration level, frequency and duration of exposure.

3.4. Airborne infection risk assessment

Respiratory infectious diseases can be transmitted through the inhalation of droplet nuclei [26], which can be suspended in air and remain airborne for prolonged periods. It has been proved that both emerging (such as SARS, severe acute respiratory syndrome) and re-emerging (such as TB, tuberculosis) respiratory infections can be spread by the airborne route. The outbreak of SARS and the pending flu pandemic called for more understanding of the airborne transmission mechanism. During the dispersion process, the transient concentrations can be significantly higher than the mean concentrations. For the prevention and control of airborne infection transmission, it is therefore necessary to estimate the practical impact induced by the instantaneous peak concentrations within a time scale as small as one inhalation period. A widely used infection risk assessment model, i.e. the Wells–Riley model, was employed to estimate the probability of airborne transmission of an infectious disease due to this kind of cross-contamination [27]:

$$P = \frac{C}{S} = 1 - \exp\left(-\frac{Iqpt}{Q}\right) \quad (1)$$

where P is the probability of infection, C the number of infection cases, S the number of susceptibles, I the number of infectors, p the pulmonary ventilation rate of a person, q the quanta generation rate, t the exposure time interval, and Q the room ventilation rate. Exposure to one quantum of infection gives an average probability of 63% $(1 - e^{-1})$ of becoming infected. This equation can incorporate spatially distributed infection risk by conducting tracer gas measurements. Assuming that the tracer gas is released from the location of the infector (source position), the concentration at the location of each susceptible person can be measured, allowing

Table 3
The 90th percentile normalized by source concentration (source located on the 6th floor, with closed windows).

Floor	$\theta = 0^\circ$				$\theta = 180^\circ$				$\theta = 45^\circ$				$\theta = 90^\circ$			
	P1	P2	P3	P4	P1	P2	P3	P4	P1	P2	P3	P4	P1	P2	P3	P4
3	1.0	0.9	1.0	1.0	0.0	0.0	0.0	0.0	1.0	0.8	0.6	0.6	1.5	1.3	1.5	1.5
4	1.2	1.2	1.3	1.4	0.9	1.2	1.3	1.6	1.4	1.1	1.0	0.9	1.6	1.6	2.3	2.4
5	1.6	2.0	2.5	2.9	0.7	0.8	2.0	3.8	1.8	1.8	1.7	1.3	2.4	2.7	5.2	6.1
6	3.6	4.2	5.6	5.2	6.1	1.6	7.1	10.3	4.5	4.3	3.8	3.7	2.9	2.9	7.0	11.9
7	1.7	2.4	2.7	2.7	1.6	2.7	4.6	6.8	2.1	1.9	1.5	1.2	1.6	1.8	2.9	4.2
8	1.1	1.3	1.2	1.3	1.7	2.0	2.2	3.8	1.1	0.8	0.6	0.6	0.8	0.6	0.6	0.5
9	0.6	1.0	0.8	0.8	1.6	1.6	1.8	2.4	0.9	0.6	0.4	0.4	0.2	0.1	0.2	0.2

Table 4
Infection risk probabilities calculated by instantaneous peak concentration values (source located on the 6th floor with open windows).

Floor	$\theta = 0^\circ$ (in %)				$\theta = 180^\circ$ (in %)				$\theta = 45^\circ$ (in %)				$\theta = 90^\circ$ (in %)			
	P1	P2	P3	P4	P1	P2	P3	P4	P1	P2	P3	P4	P1	P2	P3	P4
3	0.01	0.01	0.01	0.01	0.01	0.02	0.00	0.01	0.01	0.01	0.01	0.01	0.01	0.01	0.01	0.02
4	0.01	0.01	0.01	0.01	0.01	0.02	0.02	0.02	0.01	0.01	0.01	0.01	0.01	0.01	0.02	0.02
5	0.02	0.02	0.02	0.01	0.01	0.02	0.03	0.03	0.02	0.02	0.01	0.02	0.01	0.01	0.02	0.03
6	0.10	0.05	0.03	0.02	0.07	0.03	0.04	0.04	0.08	0.05	0.02	0.02	0.05	0.02	0.03	0.04
7	0.02	0.03	0.02	0.02	0.02	0.04	0.03	0.03	0.02	0.02	0.01	0.01	0.01	0.02	0.02	0.03
8	0.01	0.01	0.01	0.01	0.01	0.02	0.02	0.02	0.01	0.01	0.00	0.00	0.01	0.01	0.01	0.02
9	0.01	0.01	0.01	0.01	0.01	0.02	0.02	0.02	0.00	0.01	0.00	0.00	0.00	0.00	0.01	0.01

the derivation of spatial distribution of infection risk. Here using the experimental results, the infection risk at each measurement location can be estimated based on instantaneous peak concentration values derived from 2 s-averaged (prototype) data, and the corresponding exposure time is 2 s. This is to estimate the potential risk induced by instantaneous peak concentration presented during one inhalation period of humans (2 s).

In view of the high peak-to-mean ratio under open-window conditions, as shown in Fig. 7, the following results are calculated by the data obtained when the source was located on the 6th floor under open-window condition. ASHRAE [28] recommends that the outdoor air requirements are 0.03 L/s m^2 in residential buildings over three stories, which is assumed as the constant room ventilation rate for the present study. Supposing a hypothetical measles outbreak with a high value for quantum generation rate at the source location, $q = 570$/h [29], pulmonary ventilation rate at 0.6 m^3/h [30], the calculated infection probabilities are listed in Table 4. It can be seen that the probabilities calculated by instantaneous peak concentration values are under 0.1% in all the positions for the presented cases. This suggests that the infection risk caused by instantaneous peak concentration can be neglected. Although the peak concentration value can be clearly higher than the mean value, the risk is still significantly low due to the extremely short exposure time. Furthermore, using gas phase surrogate in the risk assessment considers all the aerosols to be suspended and inhalable, and also ignores the deposition of particles. The infection risk values calculated here can be expected to overestimate the risk level, compared with that of using respiratory infectious particles.

4. Conclusions

The development of modern society calls for a greater understanding of pollutant transportation within complex building environments. To have a better understanding of air pollutant dispersion processes around high-rise residential buildings, a series of wind tunnel experiments were designed and performed under different configurations. In this paper, features of concentration fluctuations were thoroughly examined from two points of view: first to check the turbulent fluctuation characteristics of wind-induced cross-contamination and second from a practical point of view to illustrate the practical impact of concentration fluctuations.

With regard to the fluctuation characteristics of the dispersion process, we found that for most of the points studied, the values of the concentration fluctuation intensity were greater than 1, suggesting that fluctuations in instantaneous concentration are at least of the same values as the actual mean concentrations. It is therefore necessary to estimate not only the mean concentration but also the concentration fluctuations. It was also found that variations in fluctuation intensity are quite sensitive to both the source location and the wind direction. Moreover, as the CDF curves show, even in locations where the mean concentration values are relatively low, the investigation of concentration fluctuations is still important as gas entrainment could be very intermittent and sudden peaks in concentrations may occur, probably followed by long periods of near-zero concentration.

To examine the features of concentration fluctuations from a practical point of view, an averaging time of 2 s was applied on the time series of concentration in order to analyse the "instantaneous" concentration level over a time scale related to human breath. The temporal behaviour of the dispersion process was captured over a time scale as small as one inhalation period. With regard to odour assessment, the 90th percentile values give a clearer indication of where the high peak values occur than the intensity does, and it was found that the instantaneous peak concentration level can be strong enough to lead to an experience of odour annoyance. With regard to infection risk assessment, although the peak concentration values are much higher than mean values, the infection risks calculated by peak concentration values can still be neglected. Under the scenario of highly infectious agents such as measles, the infection probabilities are still under 0.1%, indicating the peak concentration values are not significant for airborne infection risk assessment.

Fluctuation behaviours during the hazardous gas dispersion process around a high-rise building due to wind effects were comprehensively discussed herein. The study is focused on the vertical dispersion characteristics within high-rise buildings. The dispersion characteristics could be different if the building was low. From the fluctuation characteristics illustrated in this study, it is not adequate to examine the mean concentration field alone, and fluctuating concentrations should be examined when evaluating potential risks. The results can be used to identify the regions of the flow where ignition could have taken place under an accidental release of flammable gas. Emergency ventilation strategies such as positive pressure ventilation (PPV) should be developed to control this kind of accidental release. Based on the odour assessment, more targeted and more effective intervention should be designed to improve the building environment. Possible optimal strategies such as using central stack or individual mechanical ventilation can be useful to minimize such cross-contamination. The experimental data presented in this study can also be used to validate the CFD models in the future work, so that the airflow and dispersion can be examined in more detail via computational methods. It is hoped that the valuable data set provided in this study will prove a useful basis for future HRR building environment research, shedding light on more effective and practical methods for pollution control and leading to improvements in urban air quality modelling and assessment.

Acknowledgements

The authors would like to thank Dr. Peter A. Hitchcock and his technical staff of CLP Wind Tunnel, Hong Kong University of Science and Technology in preparing the scaled models and assisting in

the wind tunnel tests. The project is funded by Internal Research Funding G-YJ51, PolyU.

References

[1] J.E. Cermak, Dispersion of pollutants in the urban environment, in: ASCE Spring Convention and Exhibition, vol. 3269, Pittsburgh, PA, 1978, p. 29 (preprint).
[2] S.R. Hanna, J. White, Y. Zhou, Observed winds, turbulence, and dispersion in built-up downtown areas in Oklahoma City and Manhattan, Bound.-Layer Meteorol. 125 (2007) 441–468.
[3] S.R. Hanna, M.J. Brown, F.E. Camelli, S.T. Chan, W.J. Coirier, S. Kim, O.R. Hansen, A.H. Huber, R.M. Reynolds, Detailed simulations of atmospheric flow and dispersion in downtown Manhattan: an application of five computational fluid dynamics models, Bull. Am. Meteorol. Soc. 87 (2006) 1713–1726.
[4] S.R. Hanna, O.R. Hansen, M. Ichard, D. Strimaitis, Computational Fluid Dynamics (CFD) model simulations of dispersion from chlorine railcar releases in industrial and urban areas, Atmos. Environ. 43 (2009) 262–270.
[5] M. Pontiggia, M. Derudi, M. Alba, M. Scaioni, R. Rota, Hazardous gas releases in urban areas: assessment of consequences through CFD modeling, J. Hazard. Mater. 176 (2010) 589–596.
[6] R.N. Meroney, Wind tunnel and numerical simulation of pollution dispersion: a hybrid approach, in: Croucher Advanced Study Institute on Wind Tunnel Modeling, Hong Kong University of Science and Technology, 2004 (invited lecture).
[7] K.T. Bogen, F.J. Gouveia, Impact of spatiotemporal fluctuations in airborne chemical concentration on toxic hazard assessment, J. Hazard. Mater. 152 (2008) 228–240.
[8] A.G. Venetsanos, T. Huld, P. Adams, J.G. Bartzis, Source, dispersion and combustion modelling of an accidental release of hydrogen in an urban environment, J. Hazard. Mater. 105 (2003) 1–25.
[9] E. Yee, C.A. Biltoft, Concentration fluctuation measurements in a plume dispersing through a regular array of obstacles, Bound.-Layer Meteorol. 111 (2004) 363–415.
[10] R.M. Gailis, A. Hill, A wind-tunnel simulation of plume dispersion within a large array of obstacles, Bound.-Layer Meteorol. 119 (2006) 289–338.
[11] M. Pavageau, M. Schatzmann, Wind tunnel measurements of concentration fluctuations in an urban street canyon, Atmos. Environ. 33 (1999) 3961–3971.
[12] I. Mavroidis, R.F. Griffths, Investigation of building-influenced atmospheric dispersion using a dual source technique, Environ. Monit. Assess. 65 (2000) 239–247.
[13] K. Sada, A. Sato, Numerical calculation of flow and stack-gas concentration fluctuation around a cubical building, Atmos. Environ. 36 (2002) 5527–5534.
[14] I. Mavroidis, S. Andronopoulos, J.G. Bartzis, R.F. Griffiths, Atmospheric dispersion in the presence of a three-dimensional cubical obstacle: modelling of mean concentration and concentration fluctuations, Atmos. Environ. 41 (2007) 2740–2756.
[15] S. Aubrun, B. Leitl, Unsteady characteristics of the dispersion process in the vicinity of a pig barn. Wind tunnel experiments and comparison with field data, Atmos. Environ. 38 (2004) 81–93.
[16] H.L. Higson, R.F. Griffiths, C.D. Jones, D.J. Hall, Flow and dispersion around an isolated building, Atmos. Environ. 30 (1996) 2859–2870.
[17] J.M. Santos, R.F. Griffiths, I.D. Roberts, N.C. Reis Jr., A field experiment on turbulent concentration fluctuations of an atmospheric tracer gas in the vicinity of a complex-shaped building, Atmos. Environ. 39 (2005) 4999–5012.
[18] J.L. Niu, T.C.W. Tung, On-site quantification of re-entry ratio of ventilation exhausts in multi-family residential buildings and implications, Indoor Air 18 (2008) 12–26.
[19] X.P. Liu, J.L. Niu, K.C.S. Kwok, J.H. Wang, B.Z. Li, Local characteristics of cross-unit contamination around high-rise building due to wind effect: mean concentration and infection risk assessment, J. Hazard. Mater. 192 (2011) 160–167.
[20] Australian Standard, Minimum Design Loads on Structures, AS1170.2-1989, 1989.
[21] Dispersion around buildings, in: N. Isyumov (Ed.), Wind Tunnel Studies of Buildings and Structures, ASCE Manuals and Reports on Engineering Practice No. 67, American Society of Civil Engineers, Reston, VA, 1999, pp. 137–142 (chapter 7).
[22] Building (Planning) Regulations. Laws of Hong Kong. The Hong Kong SAR Government, HK, 1997 (chapter 123F).
[23] K.R. Mylne, The vertical profile of concentration fluctuations in near-surface plumes, Bound.-Layer. Meteorol. 65 (1993) 111–136.
[24] M.F. Yassin, M. Ohba, H. Tanaka, Experimental study on flow and gaseous diffusion behind an isolated building, Environ. Monit. Assess. 147 (2008) 149–158.
[25] N.S. Dixon, A.S. Tomlin, A Lagrangian stochastic model for predicting concentration fluctuations in urban areas, Atmos. Environ. 41 (2007) 8114–8127.
[26] American Society of Heating, Refrigerating and Air-Conditioning Engineers (ASHRAE), ASHRAE Position Document on Airborne Infectious Diseases, ASHRAE, Atlanta, GA, 2009.
[27] E.C. Riley, G. Murphy, R.L. Riley, Airborne spread of measles in a suburban elementary school, Am. J. Epidemiol. 107 (1978) 421–432.
[28] American Society of Heating, Refrigerating and Air-conditioning Engineers, ASHRAE Standard 62-2007, Ventilation for Acceptable Indoor Air Quality, 2007.
[29] S.N. Rudnick, D.K. Milton, Risk of indoor airborne infection transmission estimated from carbon dioxide concentration, Indoor Air 13 (2003) 237–245.
[30] N.P. Gao, J.L. Niu, M. Perino, P. Heiselberg, The airborne transmission of infection between flats in high-rise residential buildings: tracer gas simulation, Build. Environ. 43 (2008) 1805–1817.